J. Coat. Technol. Res., **17** (3) 765–776, 2020
https://doi.org/10.1007/s11998-020-00324-5

A multifunctional antifog, antifrost, and self-cleaning zwitterionic polymer coating based on poly(SBMA-co-AA)

Weirong Zou, Zhuizhui Fan, Shixiong Zhai, Siwei Wang, Bi Xu, Zaisheng Cai

Abstract In this work, a multifunctional coating was developed by grafting a zwitterionic poly[2-(methacryloyloxy)ethyl]dimethyl-(3-sulfopropyl)-co-acrylic acid [poly(SBMA-co-AA)] polymer onto a glass slide, which possesses excellent antifog, antifrost, and self-cleaning properties. These properties are attributed to the strong hydration of the hydrophilic zwitterionic PSBMA segments. The durability of the coating can be improved because the carboxyl group (–COOH) of the PAA segment enables formation of a robust covalent bond with the amino group ($–NH_2$) on the substrate. The coating presents long-term stability, as proved by water contact angles, which were stable at $12 \pm 1°$ after exposing the coating in ambient environment for 60 days or immersing in deionized water for 24 h. In addition, the underwater oil contact angle measurement demonstrated that an oil stain on the zwitterionic poly(SBMA-co-AA) polymer coating can be easily removed upon contact with water, showing self-cleaning performance. These properties verified that the zwitterionic multifunctional coating exploited in this research has many potential application prospects, including construction, automotive, aerospace, shipbuilding, biomedical, and other optical fields.

W. Zou, Z. Fan, S. Zhai, S. Wang, B. Xu,
Z. Cai (✉)
Key Lab of Science and Technology of Eco-Textile, Ministry of Education, College of Chemistry, Chemical Engineering and Biotechnology, Donghua University, Shanghai 201620, People's Republic of China
e-mail: zshcai@dhu.edu.cn

W. Zou
e-mail: 80668627@qq.com

W. Zou, Z. Fan, S. Zhai, S. Wang, B. Xu,
Z. Cai
College of Chemistry, Chemical Engineering and Biotechnology, Donghua University, Shanghai 201620, People's Republic of China

Graphic abstract

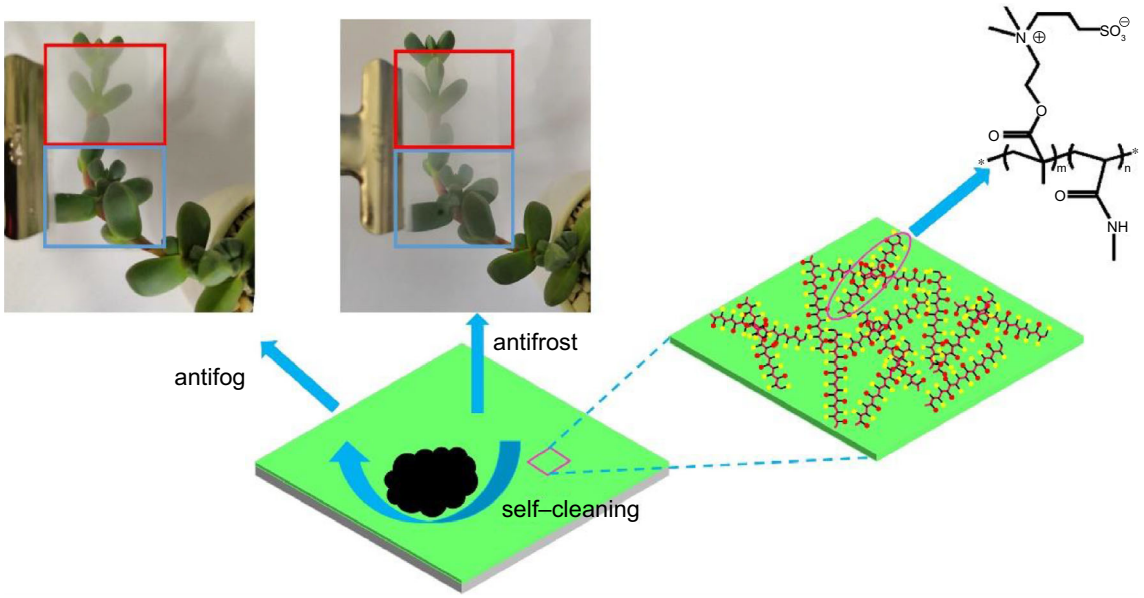

Keywords Antifog, Antifrost, Self-cleaning, Multifunctional, Zwitterionic PSBMA, Durability

Introduction

The formation of fog is attributed to uneven condensation of water droplets on the surface of transparent substrates caused by temperature and humidity change, which can significantly reduce the transparency of the substrate, such as windshields, eyeglasses, goggles, and endoscopes.[1–3] This will not only bring inconvenience to daily life but will also lead to potential dangers.[4–7] Therefore, maintaining the transparency of the substrates is essential for their practical applications. Thus far, there are two main antifogging strategies to mitigate the problems. The first method aims at controlling environmental parameters, such as temperature, relative humidity, and surrounding air flow to avoid condensation.[8–12] The second category focuses on changing the morphology of water drops by tuning the wetting characteristic of the transparent substrate surface, including adjusting the substrate's surface features (chemistry and roughness) or coating deposition.[13,14] In recent years, coating treatments have been extensively investigated in antifog fields due to their low cost, adjustable wettability, availability, and crosslink ability. According to the antifog mechanism of the coating, the antifog coating can be roughly classified into two types: hydrophobic antifog coating and hydrophilic antifog coating.

Compared with the hydrophobic coating, the hydrophilic or even superhydrophilic films have been extensively reported as antifog coatings for transparent substrates.[2,15–19] That is the reason that water droplets can spread quickly on these surfaces, forming a liquid film that can effectively reduce light scattering to avoid the formation of fog.[20–23] For example, Zhao et al. fabricated an excellent antifogging/antimicrobial coating by spin-coating the partially quaternized poly [2-(dimethylamino)ethyl methacrylate-co-methyl methacrylate] on the surface of glass slides. The excellent antifogging performance of the coating was mainly due to the hydrophilic/hydrophobic balance of the partially quaternized co-polymer, while the strongly antimicrobial performance was attributed to quaternary ammonium compound.[24] Manabe et al. designed a multifunctional antifog coating by alternately depositing poly(allylamine hydrochloride)–poly(vinyl alcohol)–poly(acrylic acid) (PAH–PVA–PAA) blend as a cationic solution and poly(vinyl alcohol)–poly(acrylic acid) (PVA–PAA) blend as an anionic solution. These coatings displayed excellent antireflection and antifogging properties, which were mainly attributed to the strong hydrophilicity of PVA.[25]

Another crucial factor that affects the performance of transparent optical materials is the surface fouling. To solve this problem, various hydrophilic materials have been studied as antifouling coatings, such as poly(*N*-vinylpyrrolidone), poly(ethylene glycol) (PEG), and zwitterionic polymers. Stains can be evidently reduced on the surfaces of these coatings, which were attributed to the water layer on the coatings by interacting with water molecules.

Zwitterionic polymers have equal anionic and cationic groups in the molecular chain, making the polymer electrically neutral. There is a strong dipole–dipole interaction between molecular segments.[26,27] Typical cations are quaternized ammonium, and zwitterionic groups can be classified into sulfobetaine (SB), carboxybetaine (CB), and phosphorylcholine (PC)

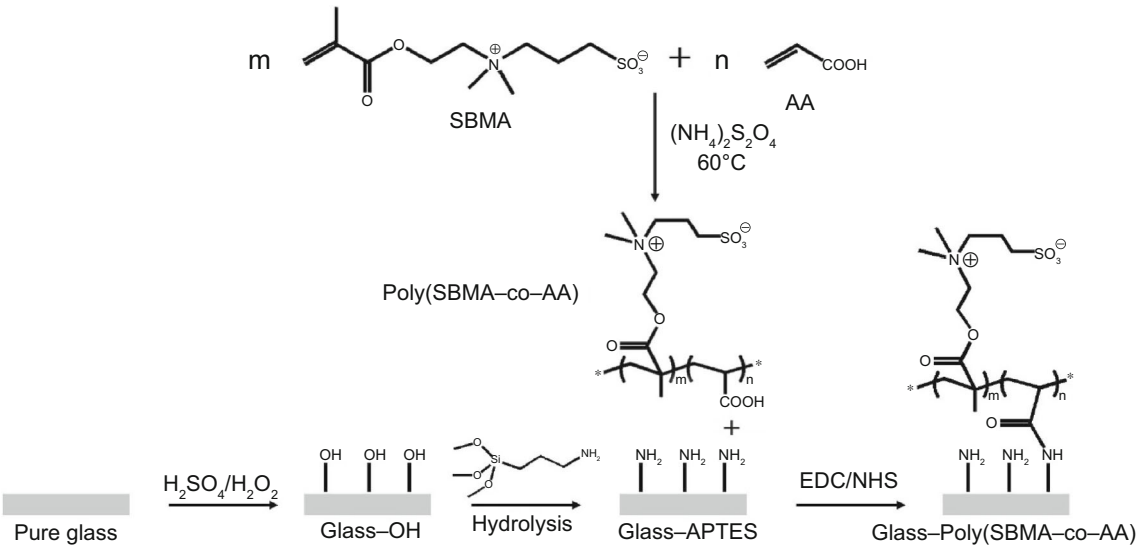

Scheme 1: Synthesis procedure of the poly(SBMA-co-AA) coating

according to the kind of anions. This special molecular structure makes it suitable for many aspects, such as emulsifiers and antifoulants.[28] These zwitterionic polymers that exhibit highly hydrophilic and antifouling performance are also attributed to their equal anionic and cationic groups on the molecular chain. In recent years, zwitterionic polymers have also been developed to achieve effective antifogging and frost-resisting for their high hydrophilicity. For instance, Huang et al. prepared a superhydrophilic coating by grafting zwitterionic sulfobetaine silane (SBSi) on oxidized surfaces. This coating displayed excellent antifog and self-cleaning performance due to the strong water–substrate interaction.[16] Li et al. fabricated a semi-interpenetrating polymer network (SIPN) coating from amphiphilic block co-polymers of polyhedral oligomeric (POSS-PDMAEMA-b-PSBMA) with a small amount of ethylene glycol dimethacrylate (EGDMA) via UV-curing. The prepared coating displayed excellent antifogging performance mainly as the hygroscopicity of PDMAEMA and PSBMA blocks in SIPN.[29]

In this work, we first created a multifunctional coating based on the zwitterionic polymer poly [(2-(methacryloyloxy)ethyl]dimethyl-(3-sulfopropyl)-co-acrylic acid [poly(SBMA-co-AA)]. This coating can achieve antifog, antifrost, and self-cleaning properties at the same time. Moreover, the coating also exhibits distinguished long-term durability and water resistance. Therefore, this strategy would be expected to address the problems of single function, poor water resistance, and durability of the current antifog coatings. This kind of zwitterionic multifunctional coating can be obtained by a simple preparation method: (1) pretreatment of glass slide with (3-aminopropyl)triethoxysilane (APTES); (2) synthesis of poly(SBMA-co-AA); (3) grafting poly(SBMA-co-AA) onto glass slide.

Materials and methods

Materials

[2-(Methacryloyloxy)ethyl]dimethyl-(3-sulfopropyl) (SBMA, ≥ 97%), ammonium persulfate (APS, AR, ≥ 98%), 3-aminopropyl triethoxysilane (APTES,99%), *N*-(3-dimethylaminopropyl)-*N*′-ethylcarbodiimide hydrochloride (EDC, 98%), *N*-hydroxysuccinimide (NHS, 98%), and 2-(*N*-morpholino)ethanesulfonic acid (MES, ≥ 99%) were purchased from Aladdin. Sulfuric acid (H_2SO_4, AR, 98 wt%), hydrogen peroxide (H_2O_2, AR, 30 wt%), tetrahydrofuran (THF, AR), acetone (C_3H_6O, AR), ethanol (C_2H_5OH, AR), acrylic acid (AA, AR), disodium hydrogen phosphate dodecahydrate (AR, ≥ 99.0%), and sodium dihydrogen phosphate dihydrate (AR, ≥ 99.0%) were purchased from Shanghai Sinopharm Reagent Company (China).

Pretreatment of glass slide

In order to obtain enough active functional groups on the surface of the pure glass slide, APTES was grafted onto its surface by silanization, as shown in Scheme 1. The glass slides (24 × 24 mm^2) were continuously washed with deionized water, acetone, and ethanol for 30 min in an ultrasonic cleaner. They were hydroxylated by immersion in a piranha solution (H_2SO_4: H_2O_2 = 7:3) at 90°C for 1 h and then washed with copious amounts of deionized water and ethanol to neutrality. The hydroxylated slides were immersed in an APTES solution (5 mL APTES, 92 mL methanol, and 3 mL water) overnight at room temperature to obtain the amination glass (glass-APTES) slides. After that, deionized water and ethanol were used to wash the glass-APTES slides thoroughly; then, the glass-

APTES slides were dried at 60°C in a vacuum oven for further use.

Synthesis of poly(SBMA-co-AA)

The zwitterionic poly(SBMA-co-AA) polymer was synthesized via free-radical-initiated polymerization method. In a three-necked flask, 6.3 g SBMA and 1.08 g AA were dissolved with 40 mL deionized water. Then, 0.06 g ammonium persulfate was dissolved in 10 mL deionized water and transferred to a 10 mL syringe. Under stirring at 60°C, it was dropped into the reaction system as the initiator in the N_2 atmosphere. After continuous reaction for 6 h, the mixed solution was precipitated with THF solution for two times at room temperature. Then, the zwitterionic poly(SBMA-co-AA) polymer product was obtained by freeze-drying.

Grafting poly(SBMA-co-AA) onto glass slide

The zwitterionic poly(SBMA-co-AA) polymer (6.3 g) was dissolved in 50 mL of 0.1 M MES buffer. Then, EDC (1.8 g, 0.2 mol) and NHS (1.1 g, 0.1 mol) were added to the solution and stirred for 1 h. After that, the amination glass slides were soaked in the above solution for 24 h to obtain the zwitterionic poly (SBMA-co-AA)-modified glass [glass-poly(SBMA-co-AA)] slides. Finally, the glass-poly(SBMA-co-AA) slides were washed thoroughly with deionized water and dried at 60°C in a vacuum oven.

Characterizations

^{1}H NMR spectra were conducted with an AV400 M ^{1}H NMR spectrometer with tetramethylsilane (TMS) as an internal standard. The ^{1}H NMR sample was prepared by dissolving zwitterionic poly(SBMA-co-AA) polymer into D_2O. The molecular weight of poly(SBMA-co-AA) was determined by PL50 gel permeation chromatography (GPC) (American). Thermal gravimetric analysis (TGA) was obtained by a TG209F1 instrument (Germany) under nitrogen atmosphere. Fourier transform infrared (FTIR) spectroscopy was carried out on a PerkinElmer Spectrum Two spectrometer (American). The surface chemical composition of the glass-poly(SBMA-co-AA) slide was characterized by X-ray photoelectron spectroscopy (XPS). The XPS analysis was performed using a Thermo ESCALAB 250 spectrometer (American) with a monochromatic Al Kα source at 1486.6 eV. The topography of the surfaces was measured by a tapping-mode atomic force microscope (AFM) with an MFP-3D microscope (Asylum Research, USA) at room temperature. The water contact angles (WACs) of the glass-poly(SBMA-co-AA) slide surface and their development were recorded by the sessile-drop method, using an optical CA goniometer (KRÜSS Contact Angle DSA30R, KRÜSS, Germany) at ambient temperature; the volume of droplets was 5 μL. The average water CAs were obtained at three different positions on the samples to characterize the average wetting properties of the coatings. UV–Vis spectrophotometer (UV-3600, Jasco) was used to measure the UV–Vis transmission spectra of glass-poly(SBMA-co-AA) slide.

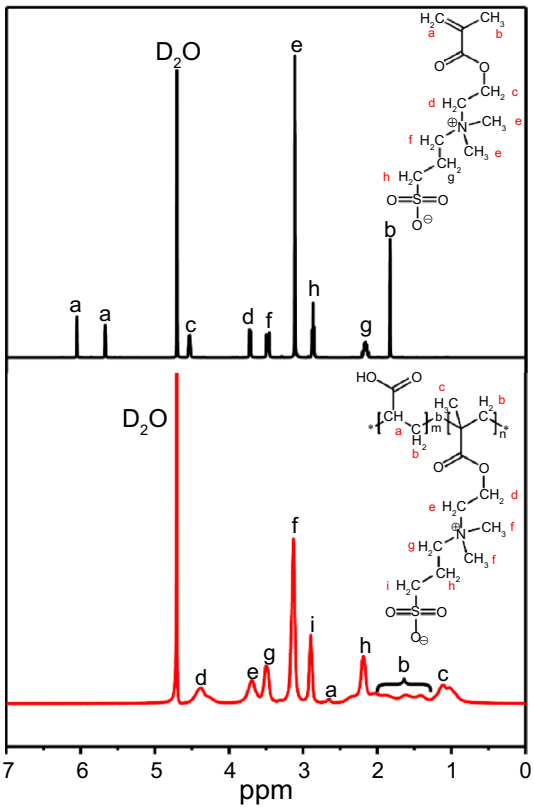

Fig. 1: ^{1}H NMR spectra of SBMA and poly (SBMA-co-AA)

Antifog and antifrost tests

The hot bath and freezing methods were used to evaluate the antifog and antifrost properties, respectively. For the antifog test, the glass-poly(SBMA-co-AA) slide and the pure glass slide were set above the hot bath (80°C) for 10 s; the distance between the hot bath and the samples was 5 cm. The fogging performances were recorded after removing samples immediately from the water steam. The glass-poly(SBMA-co-AA) slide and the pure glass slide were stored in a freezer at − 18°C for 30 min, and then, they were exposed to ambient conditions to estimate the antifrost performance. Furthermore, in order to quantitatively evaluate the antifog and frost-resisting properties of the glass-poly(SBMA-co-AA) slides, light transmissions in the range of 380–780 nm were recorded during the fogging or frosting tests.

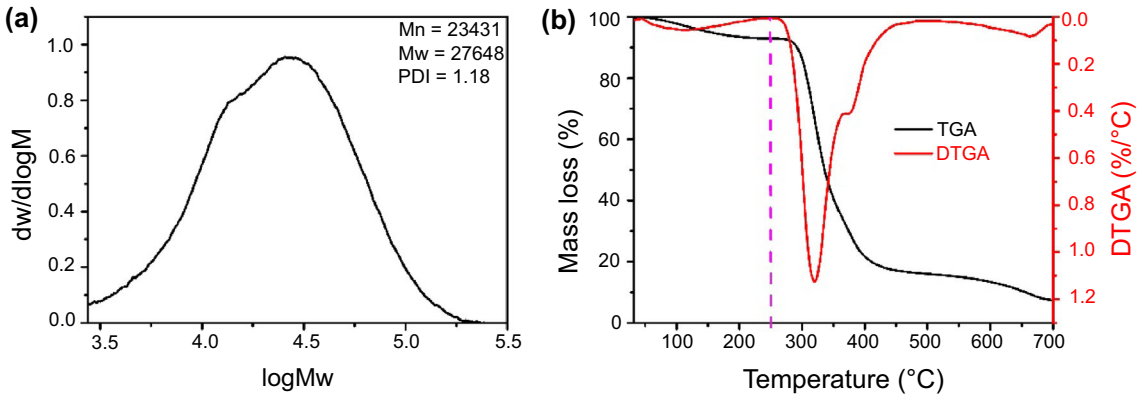

Fig. 2: (a) GPC curve of zwitterionic polymer poly(SBMA-co-AA); (b) TGA and DTGA spectra of zwitterionic polymer poly(SBMA-co-AA)

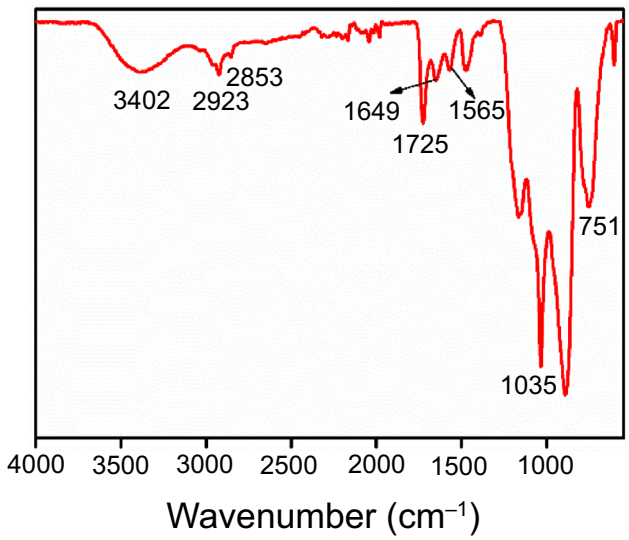

Fig. 3: FTIR spectrum of the surface of glass-poly(SBMA-co-AA) slide

Stability tests

The durability of the zwitterionic poly(SBMA-co-AA) coating was investigated through exposing the glass-poly(SBMA-co-AA) slide in the surrounding environment for 60 days or immersing in deionized water for 24 h. The durability of the poly(SBMA-co-AA) coating was evaluated by continuously monitoring the change of the contact angle and the antifogging and antifrost properties. These samples were dried in a vacuum oven at 60°C after each test.

Self-cleaning tests

To verify the self-cleaning property of the zwitterionic poly(SBMA-co-AA) coating, a hydrophobic contaminant mixed with soybean oil and carbon powder was dropped on the pure glass slide and the glass-poly(SBMA-co-AA) slide, respectively. The removal effects of the stains were characterized by continuously rinsing samples with water.

Results and discussion

Preparation and properties of the poly(SBMA-co-AA) coating

The ^{1}H NMR spectra of SBMA and the zwitterionic poly(SBMA-co-AA) polymer are shown in Fig. 1. δ = 4.7 ppm was the solvent peak of D_2O. The proton absorption peaks of SBMA were presented as follows: δ = 6.05 ppm and δ = 5.67 ppm were the characteristic proton absorption peaks of (–C=CH_2); δ = 4.54 ppm was the proton absorption peak of methylene group on (–OCH_2–); δ = 3.45–3.73 ppm was the methylene proton absorption peak on (–$^{+}NCH_2$–) connected to N; δ = 3.1 ppm was the methyl proton absorption peak on [–$^{+}N(CH_3)_2$] connected to N; δ = 2.87 ppm was the methylene proton absorption peak on (–CH_2–SO_3^-) attached to the sulfonic acid group; δ = 2.15 ppm was a methylene proton absorption peak on (–CH_2–C–SO_3^-) separated from the sulfonic acid group by a C atom; δ = 1.83 ppm was the proton absorption peak of (–CH_3). In the ^{1}H NMR spectrum of the zwitterionic poly(SBMA-co-AA) polymer, the proton characteristic absorption peaks of δ = 6.05 ppm and δ = 5.67 ppm disappeared,[30,31] which indicated the complete polymerization of SBMA and AA.

The molecular weights of the zwitterionic polymer poly(SBMA-co-AA) were characterized by GPC. As shown in Fig. 2a, the Mw of poly(SBMA-co-AA) was 27648 and its PDI was 1.18, which indicated that the molecular weight of poly(SBMA-co-AA) was uniformly distributed. The thermal stability of the zwitterionic polymer poly(SBMA-co-AA) was examined by TGA. As shown in Fig. 2b, the zwitterionic polymer poly(SBMA-co-AA) was stable up to 250°C, which met the requirements for practical applications. In addition, there was about 7.9 wt% mass loss which was observed from 44 to 250°C, resulting from the exis-

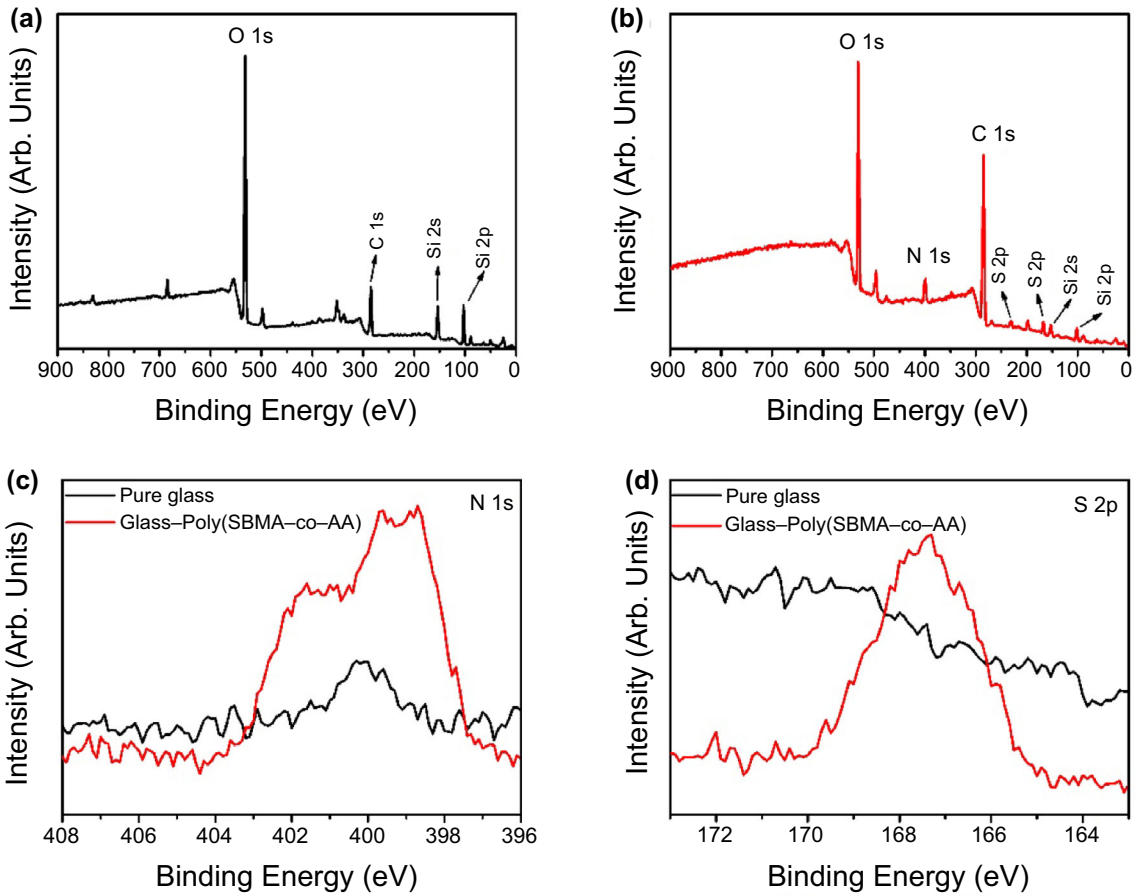

Fig. 4: XPS spectra of (a) pure glass slide; (b) glass-poly(SBMA-co-AA) slide; (c) N 1s and (d) S 2p for the pure glass slide and glass-poly(SBMA-co-AA) slide

tence of free and bound water in the zwitterionic polymer poly(SBMA-co-AA).

The FTIR spectrum of the surface of the glass-poly(SBMA-co-AA) slide is shown in Fig. 3. The zwitterionic poly(SBMA-co-AA) polymer was grafted onto a glass-APTES slide by amidation reaction. The 3402 cm^{-1} peak was caused by bound water, which was formed by the highly hydrophilic zwitterionic PSBMA segments in the poly(SBMA-co-AA) polymer. The 2923 and 2853 cm^{-1} peaks were attributed to the stretching vibration of ($–CH_3$ and $–CH_2–$).[32] The peak at 1725 cm^{-1} was assigned to the carbonyl stretching vibration. The 1649 and 1565 cm^{-1} peaks corresponded to amide groups [O=C–NH];[33] the peaks of 751 and 1035 cm^{-1} belonged to the –Si–O–Si– and –Si–O–C– stretching vibrations.[34] These results demonstrated that a robust amide bond was formed between the carboxyl group (–COOH) on the poly(SBMA-co-AA) polymer and the amino group ($–NH_2$) on the surface of the glass-APTES slide. Hence, the FTIR spectrum further indicated that the zwitterionic poly (SBMA-co-AA) polymer was successfully grafted onto the surface of glass slide.

The surface chemical composition, element contents of the substrate surface, and the changes of the chemical bond could be confirmed by X-ray photoelectron spectroscopy (XPS). The XPS spectra of the pure glass slide and the glass-poly(SBMA-co-AA) slide are shown in Fig. 4. The emergence of N and S elements was clearly observed on the surface of the glass-poly(SBMA-co-AA) slide (Fig. 4b) but did not exist on the pure glass slide surface (Fig. 4a). The N 1s peak with a binding energy of 401 eV (Fig. 4c) was attributed to the quaternary ammonium [$– N(CH_3)_2^+$].[35,36] Moreover, spin–orbit split doublets of S 2p peak were observed at the binding energy 167.0 and 168.2 eV, which were associated with the sulfonate [$–CSO_3^-$] (Fig. 4d). The characteristic S element of the zwitterionic poly(SBMA-co-AA) co-polymer was only observed on the surface of the glass-poly(SBMA-co-AA) slide, which was consistent with the ^1H NMR and FTIR results.

Atomic force microscope (AFM) with tapping mode was used to analyze the morphologies of the surfaces. The morphologies of the sample surface and the corresponding roughness values are shown in Fig. 5. The surface of pure glass slide was relatively smooth with a low roughness value (Ra = 0.54 nm in average), as shown in Fig. 5a and 5b. After amination treatment with APTES, the surface roughness value of the glass-

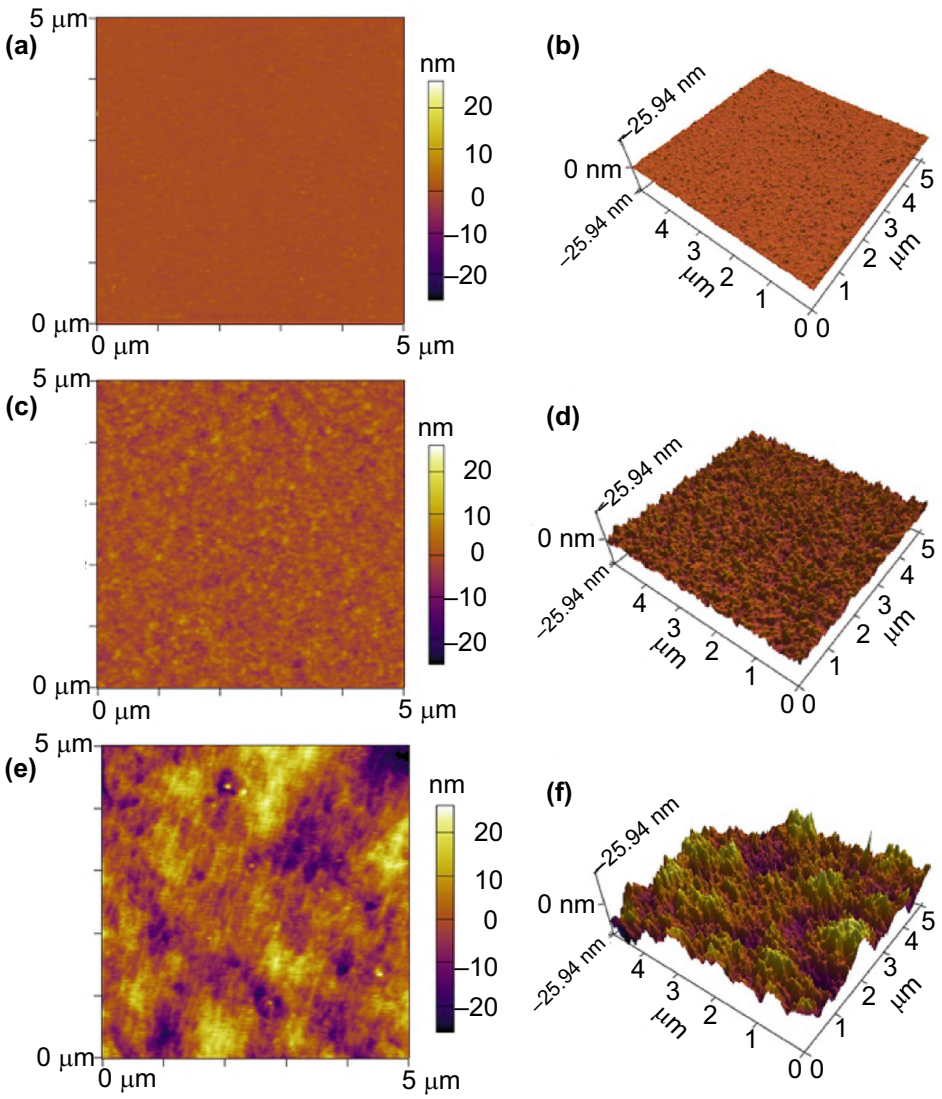

Fig. 5: Tapping-mode AFM images in air: (a, b) pure glass slide (Sa = 0.54 nm), (c, d) glass-APTES slide (Sa = 1.69 nm), and (e, f) glass-poly(SBMA-co-AA) slide (Ra = 6.12 nm)

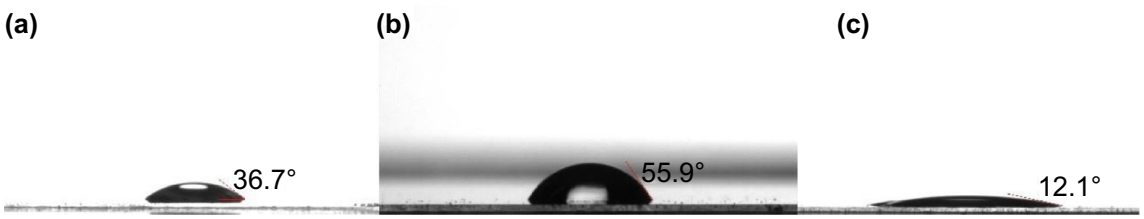

Fig. 6: Changes of water contact angle on glass slide. (a) Pure glass slide, (b) glass-APTES slide, and (c) glass-poly(SBMA-co-AA) slide

APTES slide increased to 1.69 nm on average (Fig. 5c and 5d). Finally, the glass-APTES was further modified with the zwitterionic poly(SBMA-co-AA) polymer; the surface roughness value of glass-poly(SBMA-co-AA) slide reached 6.12 nm on average (Fig. 5e and 5f). In addition, the brush poly(SBMA-co-AA) can also be observed in Fig. 5e and 5f. The final thickness of the coating reached 60 ± 0.02 nm.

The wettability of the pure glass slide and the modified glass slides was measured by a water contact angle (WCA) analyzer. The results are depicted in Fig. 6. The pure glass slide showed a WCA of 36.7° in

Fig. 6a. After modifying with the APTES, the WCA increased to 55.9° (Fig. 6b). This was due to the hydrophobicity of the silane coupling agent APTES, indicating that the pure glass slide was successfully modified by the APTES. After that, the glass-APTES was further modified with zwitterionic poly(SBMA-co-AA) polymer and the WCA decreased to only 12.1° (Fig. 6c), which was attributed to the highly hydrophilic zwitterionic PSBMA segments in the poly(SBMA-co-AA). These results indicated that zwitterionic poly (SBMA-co-AA) coating has excellent wettability.

To further investigate the wetting properties of the zwitterionic poly(SBMA-co-AA) coatings, the development of contact angle and diameter [$\Delta D = D - D_0$, D_0 was the original diameter ($t = 0$ s); D was the diameter ($t = \Delta t$ s)] of water drops with contact time on the surface of the glass-poly(SBMA-co-AA) slide was also recorded within 8 s. As shown in Fig. 7, it can be observed that the water contact angle declined rapidly to 15° on the surface of the glass-poly(SBMA-co-AA) slide within 2 s, whereas the diameter of the water droplet increased more than 25% on the surface of the glass-poly(SBMA-co-AA) slide. As the contact time increased to 4 s, the water contact angle (WCA) reached a steady state at 12 ± 1°. The diameter of the water droplet also increased by a steady state above 28 ± 1% on the glass-poly(SBMA-co-AA) slide surface. The water contact angle (WCA) and the diameter of the zwitterionic poly(SBMA-co-AA) coating surface changed quickly at the early time, which were attributed to the hydrophilic zwitterionic PSBMA segments of the poly(SBMA-co-AA) coating. This phenomenon could also explain the excellent antifog and antifrost properties of the zwitterionic poly (SBMA-co-AA) coatings.

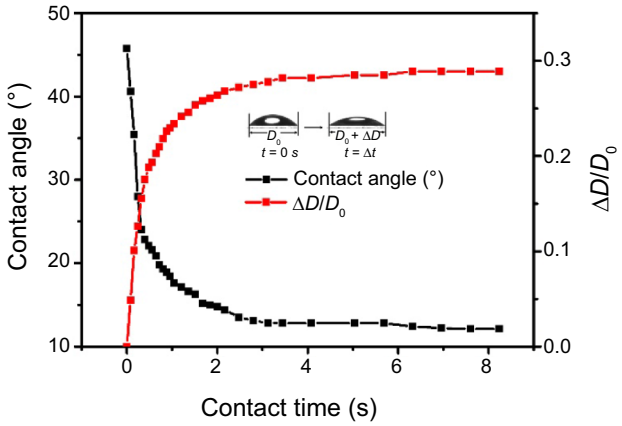

Fig. 7: Contact angle and diameter [$\Delta D = D - D_0$, D_0 was the original diameter ($t = 0$ s); D was the diameter ($t = \Delta t$ s)] vary with the contact time of the zwitterionic poly(SBMA-co-AA) coating

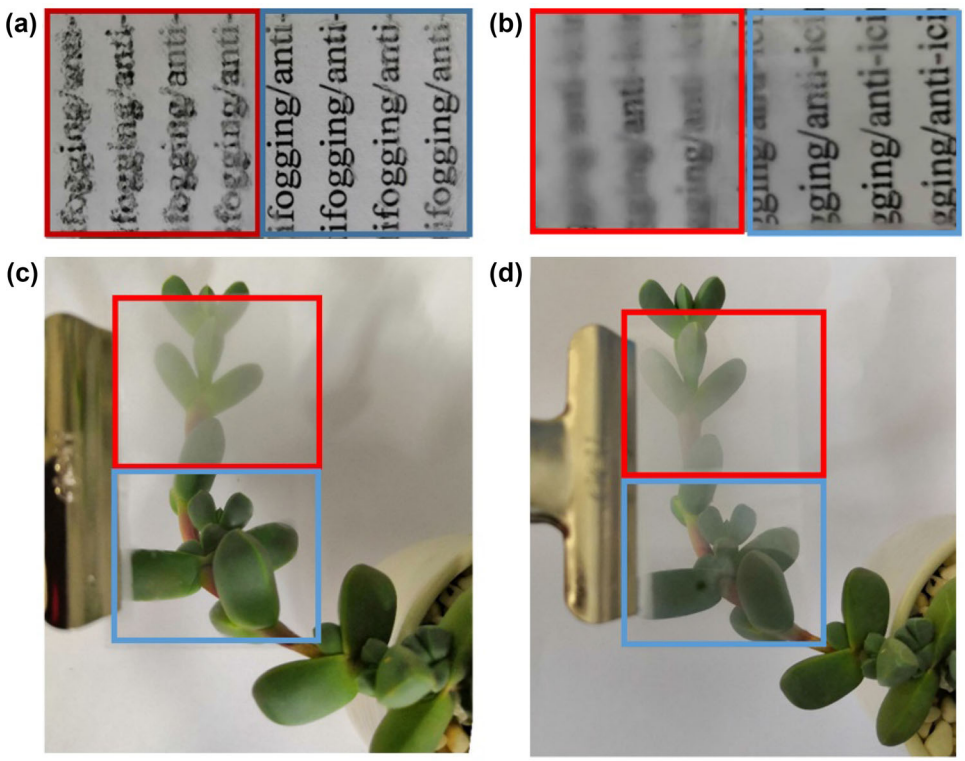

Fig. 8: Photographs of poly(SBMA-co-AA)-modified glass slides with a blue border and pure glass slides with a red border: (a) and (c) exposed the pure glass slide and the modified glass slide to about 5 cm above the hot water vapor of 80°C for 10 s; (b) and (d) the pure glass slides and the modified glass slides were stored in a refrigerator at − 18°C for 30 min

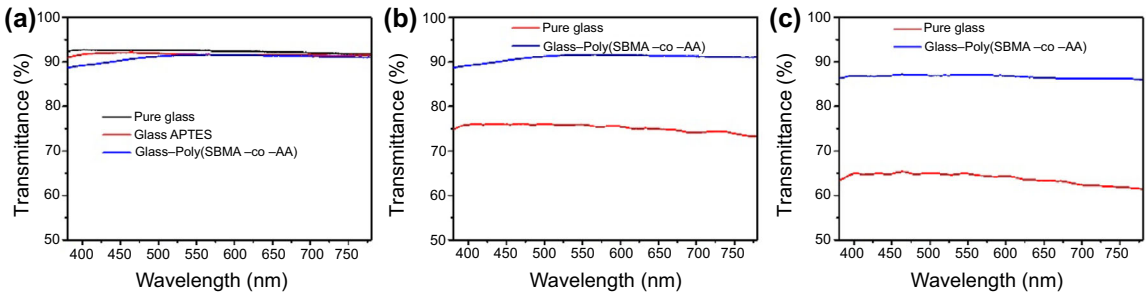

Fig. 9: Light transmission of various samples: (a) before fogging, (b) after fogging, and (c) after freezing

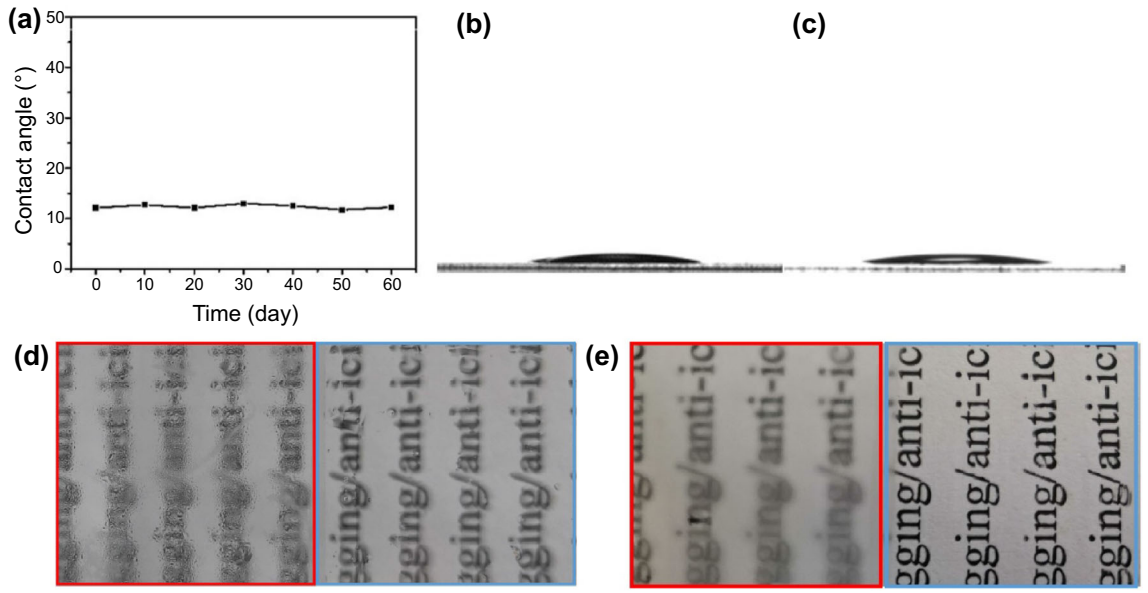

Fig. 10: (a) Water contact angle changes exposed at different times. (b) Water contact angle before soaking; (c) water contact angle after soaking for 24 h. Photographs of poly(SBMA-co-AA)-modified glass slides with a blue border and pure glass slides with a red border: (d) exposing the pure glass slide and the modified glass slide to about 5 cm above the hot water vapor of 80°C for 10 s; (e) the pure glass slides and the modified glass slides were stored in a refrigerator at − 18°C for 30 min

Antifog and antifrost performance

Good antifog and antifrost properties are critical to obtain optically clear materials. In this work, the hot water vapor and frozen storage experiments were conducted to evaluate the antifog and frost-resisting performance of the glass-poly(SBMA-co-AA) slide, respectively. The antifog and antifrost performances of the pure glass slide and the glass-poly(SBMA-co-AA) slide are shown in Fig. 8. It can be seen that a large number of water droplets accumulated on the pure glass slide after 10 s exposure to 80°C hot water vapor, while little fog formation was observed on the glass-poly(SBMA-co-AA) slide (Fig. 8a and 8c). This was because on the surface of the zwitterionic poly(SBMA-co-AA) coating, water droplets can form a liquid film quickly, which reduces light scattering to avoid the formation of fog. In addition, the pure glass slide almost completely lost its transparency owing to severe frosting, which could transform into fog after exposing to ambient conditions for 5 s (Fig. 8b and 8d).[37] On the contrary, little frost or fog was observed on the glass-poly(SBMA-co-AA) slide, still maintaining an excellent transparency. This phenomenon was attributed to the fact that water molecules from a nonfrozen bonded water can interact with the hydrophilic coating through hydrogen bonding.[38,39] In addition, the zwitterionic PSBMA segments could reduce the freezing point of water.[40]

In this work, UV–Vis spectrophotometer was used to further quantitatively measure the antifog and antifrost performances, selecting the spectral data in the range of 380–780 nm. According to the standard of American Society for Testing and Materials (ASTM) F659-06,[41] the definition of an antifog coating is one that maintains a light transmittance over 80% after

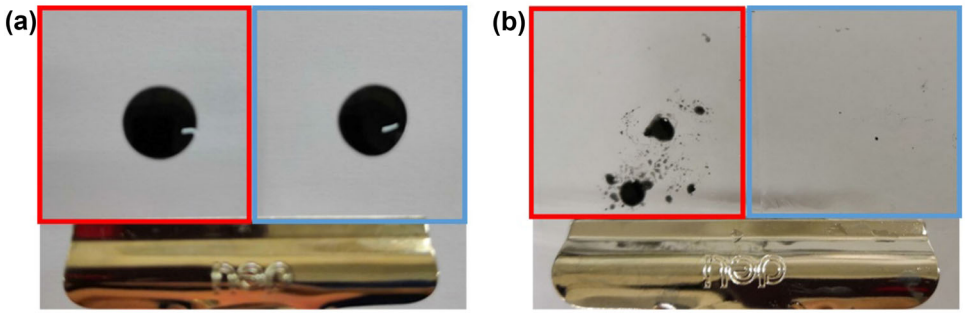

Fig. 11: Self-cleaning performance of the glass-poly(SBMA-co-AA) slides with a blue border and pure glass slides with a red border: (a) before rinsing and (b) after rinsing with water

exposure to hot water vapor for 30 s. Before the fogging and frosting tests, it could be observed that the glass-poly(SBMA-co-AA) slide exhibited similar light transmission (about 90%, Fig. 9a) with the pure glass slide. During the fogging testing, the light transmission of the pure glass slide quickly decreased to ~ 75%, while the light transmission of the glass-poly(SBMA-co-AA) slide still remained as high as ~ 88% (Fig. 9b). In addition, during the frosting testing, it could also be observed that the light transmission of the pure glass slide decreased to less than 65% owing to severe frosting on its surface, while a high transmission (~ 86%) could be observed on the glass-poly(SBMA-co-AA) slide (Fig. 9c).

Long-term stability

In practical applications, the durability of antifog coatings remains a great challenge. In this work, the long-term effectiveness of the zwitterionic poly(SBMA-co-AA) coating was evaluated by exposing it to the ambient environment for 2 months or immersing in deionized water for 24 h. There was no significant change in antifogging (Fig. 10d) or frost-resisting (Fig. 10e) properties. In addition, the results of the water contact angle test (Fig. 10a, 10b, and 10c) further demonstrated that the surface of the zwitterionic poly(SBMA-co-AA) coating was still highly hydrophilic. This effective stability was attributed to the robust covalent bonding, which formed between the carboxyl group (–COOH) in the zwitterionic poly(SBMA-co-AA) and the amino group ($–NH_2$) on the surface of the glass-APTES by amidation reaction.[42]

Self-cleaning performance

To verify the self-cleaning performance of the zwitterionic poly(SBMA-co-AA) coating, soybean oil and carbon powder were mixed as oil stains, which were dropped on the pure glass slide and the glass-poly(SBMA-co-AA) slide. Then, these contaminated slides were rinsed with water. The optical images are shown in Fig. 11, on the pure glass slide, some oil stains still remained after a continuous rinsing. On the contrary, on the glass-poly(SBMA-co-AA) slide, almost all of the oil stains were washed away.[43] Thus, the zwitterionic poly(SBMA-co-AA) coating presents an excellent repellence to oil stains because of its low adhesion to hydrophobic fluids under water.

Conclusions

In this work, we first developed a multifunctional coating with excellent antifog, antifrost, and self-cleaning properties, which were based on the zwitterionic poly(SBMA-co-AA) polymer for transparent optical substrates. The hydrophilic zwitterionic PSBMA segments made the zwitterionic poly(SBMA-co-AA) coating possess excellent antifog and frost-resisting properties. In addition, owing to the strong water–PSBMA interaction on the glass-poly(SBMA-co-AA) slide, the oil stains could be washed away easily. Further, the PAA segments formed robust covalent bonds with the amino group ($–NH_2$) on the substrate to enhance the durability of the zwitterionic poly(SBMA-co-AA) coating. Results showed that the zwitterionic poly(SBMA-co-AA) multifunctional coating developed in this research had great potential application prospects, such as construction, automotive, aerospace, shipbuilding, and biomedical.

Acknowledgments The research was financially supported by the National Key R&D Program of China (Grants 2017YFB0309405 and 2017YFB 0309103).

References

1. Di Mundo, R, d'Agostino, R, Palumbo, F, "Long-Lasting Antifog Plasma Modification of Transparent Plastics." *ACS Appl. Mater. Interfaces.*, **6** (19) 17059–17066 (2014)
2. Wang, Y, Li, T, Li, S, Sun, J, "Antifogging and Frost-Resisting Polyelectrolyte Coatings Capable of Healing

Scratches and Restoring Transparency.'' *Chem. Mater.*, **27** (23) 8058–8065 (2015)
3. Li, Y, Fang, X, Wang, Y, Ma, B, Sun, J, ''Highly Transparent and Water-Enabled Healable Antifogging and Frost-Resisting Films Based on Poly(Vinyl Alcohol)-Nafion Complexes.'' *Chem. Mater.*, **28** (19) 6975–6984 (2016)
4. San-Juan, M, Martin, O, Mirones, BJ, De Tiedra, P, ''Assessment of Efficiency of Windscreen Demisting Systems in Electrical Vehicles by Using IR Thermography.'' *Appl. Therm. Eng.*, **104** 479–485 (2016)
5. Lawrentschuk, N, Fleshner, NE, Bolton, DM, ''Laparoscopic Lens Fogging: A Review of Etiology and Methods to Maintain a Clear Visual Field.'' *J. Endourol.*, **24** (6) 905–913 (2010)
6. Piromchai, P, Kasemsiri, P, Thanaviratananich, S, ''Alternative Agents to Prevent Fogging in Head and Neck Endoscopy.'' *Clin. Med. Insights Ear Nose Throat*, **4** 1–4 (2011)
7. Cai, M-J, Li, Q-Q, Chen, X-M, ''Synthesis, Surface Activity, and Antifogging Property of Triethanolamine Monolaurate Ester.'' *Chin. J. Chem. Phys.*, **28** (2) 223–229 (2015)
8. Zhang, G, Zou, H, Qin, F, Xue, Q, Tian, C, ''Investigation on an Improved Heat Pump AC System with the View of Return Air Utilization and Anti-Fogging for Electric Vehicles.'' *Appl. Therm. Eng.*, **115** 726–735 (2017)
9. Aroussi, A, Hassan, A, Morsi, YS, ''Numerical Simulation of the Airflow Over and Heat Transfer Through a Vehicle Windshield Defrosting and Demisting System.'' *Heat Mass Transf.*, **39** (5–6) 401–405 (2003)
10. Sui, D, Huang, Y, Huang, L, Liang, J, Ma, Y, Chen, Y, ''Flexible and Transparent Electrothermal Film Heaters Based on Graphene Materials.'' *Small*, **7** (22) 3186–3192 (2011)
11. Hu, X, Yu, Y, Wang, Y, Wang, Y, Zhou, J, Song, L, ''Highly Transparent Superhydrophilic Graphene Oxide Coating for Antifogging.'' *Mater. Lett.*, **182** 372–375 (2016)
12. Kim, H-J, Kim, D-I, Kim, S-S, Kim, Y-Y, Park, S-E, Choi, G, Lee, DW, Kim, Y, ''Observation of Convection Phenomenon by High-Performance Transparent Heater Based on Pt-Decorated Ni Micromesh.'' *AIP Adv.*, **7** (2) 25 (2017)
13. Shibraen, MHMA, Yagoub, H, Zhang, X, Xu, J, Yang, S, ''Anti-Fogging and Anti-Frosting Behaviors of Layer-by-Layer Assembled Cellulose Derivative Thin Film.'' *Appl. Surf. Sci.*, **370** 1–5 (2016)
14. Tanaka, C, Shiratori, S, Fabrication of the Durable Low Refractive Index Thin Film with Chitin-Nanofiber by LBL Method. In: Goldmann, M, Guenoun, P (eds.) *ICOMF14 - 14th International Conference on Organized Molecular Films*, 2013
15. Xu, F, Li, X, Li, Y, Sun, J, ''Oil-Repellent Antifogging Films with Water-Enabled Functional and Structural Healing Ability.'' *ACS Appl. Mater. Interfaces*, **9** (33) 27955–27963 (2017)
16. Huang, K-T, Yeh, S-B, Huang, C-J, ''Surface Modification for Superhydrophilicity and Underwater Superoleophobicity: Applications in Antifog, Underwater Self-Cleaning, and Oil–Water Separation.'' *ACS Appl. Mater. Interfaces*, **7** (38) 21021–21029 (2015)
17. Xu, L, He, J, ''Antifogging and Antireflection Coatings Fabricated by Integrating Solid and Mesoporous Silica Nanoparticles Without Any Post-Treatments.'' *ACS Appl. Mater. Interfaces*, **4** (6) 3293–3299 (2012)
18. Wang, R, Hashimoto, K, Fujishima, A, Chikuni, M, Kojima, E, Kitamura, A, Shimohigoshi, M, Watanabe, T, ''Light-Induced Amphiphilic Surfaces.'' *Nature*, **388** (6641) 431–432 (1997)
19. Zhao, J, Meyer, A, Ma, L, Ming, W, ''Acrylic Coatings with Surprising Antifogging and Frost-Resisting Properties.'' *Chem. Commun.*, **49** (100) 11764–11766 (2013)
20. England, MW, Urata, C, Dunderdale, GJ, Hozumi, A, ''Anti-Fogging/Self-Healing Properties of Clay-Containing Transparent Nanocomposite Thin Films.'' *ACS Appl. Mater. Interfaces*, **8** (7) 4318–4322 (2016)
21. Brown, PS, Atkinson, ODLA, Badyal, JPS, ''Ultrafast Oleophobic–Hydrophilic Switching Surfaces for Antifogging, Self-Cleaning, and Oil Water Separation.'' *ACS Appl. Mater. Interfaces*, **6** (10) 7504–7511 (2014)
22. Wong, WSY, Nasiri, N, Rodriguez, AL, Nisbet, DR, Tricoli, A, ''Hierarchical Amorphous Nanofibers for Transparent Inherently Super-Hydrophilic Coatings.'' *J. Mater. Chem. A*, **2** (37) 15575–15581 (2014)
23. Zhao, J, Meyer, A, Ma, L, Wang, X, Ming, W, ''Terpolymer-Based SIPN Coating with Excellent Antifogging and Frost-Resisting Properties.'' *RSC Adv.*, **5** (124) 102560–102566 (2015)
24. Zhao, J, Ma, L, Millians, W, Wu, T, Ming, W, ''Dual-Functional Antifogging/Antimicrobial Polymer Coating.'' *ACS Appl. Mater. Interfaces*, **8** (13) 8737–8742 (2016)
25. Manabe, K, Matsuda, M, Nakamura, C, Takahashi, K, Kyung, K-H, Shiratori, S, ''Antifibrinogen, Antireflective, Antifogging Surfaces with Biocompatible Nano-Ordered Hierarchical Texture Fabricated by Layer-by-Layer Self-Assembly.'' *Chem. Mater.*, **29** (11) 4745–4753 (2017)
26. Liaw, DJ, Huang, CC, ''Dilute Solution Properties of Poly(3-Dimethyl Acryloyloxyethyl Ammonium Propiolactone).'' *Polymer*, **38** (26) 6355–6362 (1997)
27. Georgiev, GS, Karnenska, EB, Vassileva, ED, Kamenova, IP, Georgieva, VT, Iliev, SB, Ivanov, IA, ''Self-Assembly, Antipolyelectrolyte Effect, and Nonbiofouling Properties of Polyzwitterions.'' *Biomacromolecules*, **7** (4) 1329–1334 (2006)
28. Zheng, L, Sundaram, HS, Wei, Z, Li, C, Yuan, Z, ''Applications of Zwitterionic Polymers.'' *React. Funct. Polym.*, **118** 51–61 (2017)
29. Li, C, Li, X, Tao, C, Ren, L, Zhao, Y, Bai, S, Yuan, X, ''Amphiphilic Antifogging/Anti-Icing Coatings Containing POSS-PDMAEMA-b-PSBMA.'' *ACS Appl. Mater. Interfaces*, **9** (27) 22959–22969 (2017)
30. Tian, M, Wang, J, Zhang, E, Li, J, Duan, C, Yao, F, ''Synthesis of Agarose-*Graft*-Poly[3-Dimethyl (Methacryloyloxyethyl) Ammonium Propanesulfonate] Zwitterionic Graft Copolymers via ATRP and Their Thermally-Induced Aggregation Behavior in Aqueous Media.'' *Langmuir*, **29** (25) 8076–8085 (2013)
31. Gui, Z, Qian, J, Zhao, Q, Ji, Y, Liu, Y, Liu, T, An, Q, ''Controllable Disintegration of Temperature-Responsive Self-Assembled Multilayer Film Based on Polybetaine.'' *Colloids Surf. A Physicochem. Eng. Asp.*, **380** (1–3) 270–279 (2011)
32. Borodko, Y, Habas, SE, Koebel, M, Yang, P, Frei, H, Somorjai, GA, ''Probing the Interaction of Poly(Vinylpyrrolidone) with Platinum Nanocrystals by UV-Raman and FTIR.'' *J. Phys. Chem. B*, **110** (46) 23052–23059 (2006)
33. Nistor, M-T, Chiriac, AP, Vasile, C, Verestiuc, L, Nita, LE, ''Synthesis of Hydrogels Based on Poly(NIPAM) Inserted into Collagen Sponge.'' *Colloids Surf. B Biointerfaces*, **87** (2) 382–390 (2011)
34. Tang, M, Wang, W, Xu, D, Wang, Z, ''Synthesis of Structure-Controlled Polyborosiloxanes and Investigation on Their Viscoelastic Response to Molecular Mass of Polydimethyl-

siloxane Triggered by Both Chemical and Physical Interactions.'' *Ind. Eng. Chem. Res.*, **55** (49) 12582–12589 (2016)
35. Yeh, S-B, Chen, C-S, Chen, W-Y, Huang, C-J, ''Modification of Silicone Elastomer with Zwitterionic Silane for Durable Antifouling Properties.'' *Langmuir*, **30** (38) 11386–11393 (2014)
36. Yang, WJ, Neoh, K-G, Kang, E-T, Teo, SL-M, Rittschof, D, ''Stainless Steel Surfaces with Thiol-Terminated Hyperbranched Polymers for Functionalization via Thiol-Based Chemistry.'' *Polym. Chem.*, **4** (10) 3105–3115 (2013)
37. Sommers, AD, Truster, NL, Napora, AC, Riechman, AC, Caraballo, EJ, ''Densification of Frost on Hydrophilic and Hydrophobic Substrates—Examining the Effect of Surface Wettability.'' *Exp. Therm. Fluid Sci.*, **75** 25–34 (2016)
38. Le Tirilly, S, Tregouet, C, Bone, S, Geffroy, C, Fuller, G, Pantoustier, N, Perrin, P, Monteux, C, ''Interplay of Hydrogen Bonding and Hydrophobic Interactions to Control the Mechanical Properties of Polymer Multilayers at the Oil–Water Interface.'' *ACS Macro Lett.*, **4** (1) 25–29 (2015)
39. Xiang, F, Parviz, D, Givens, TM, Tzeng, P, Davis, EM, Stafford, CM, Green, MJ, Grunlan, JC, ''Stiff and Transparent Multilayer Thin Films Prepared Through Hydrogen-Bonding Layer-by-Layer Assembly of Graphene and Polymer.'' *Adv. Funct. Mater.*, **26** (13) 2143–2149 (2016)
40. Lee, H, Alcaraz, ML, Rubner, MF, Cohen, RE, ''Zwitter-Wettability and Antifogging Coatings with Frost-Resisting Capabilities.'' *ACS Nano*, **7** (3) 2172–2185 (2013)
41. Maechler, L, Sarra-Bournet, C, Chevallier, P, Gherardi, N, Laroche, G, ''Anti-Fog Layer Deposition onto Polymer Materials: A Multi-Step Approach.'' *Plasma Chem. Plasma Process.*, **31** (1) 175–187 (2011)
42. Gavezzotti, A, ''Comparing the Strength of Covalent Bonds, Intermolecular Hydrogen Bonds and Other Intermolecular Interactions for Organic Molecules: X-ray Diffraction Data and Quantum Chemical Calculations.'' *New J. Chem.*, **40** (8) 6848–6853 (2016)
43. Nishimoto, S, Bhushan, B, ''Bioinspired Self-Cleaning Surfaces with Superhydrophobicity, Superoleophobicity, and Superhydrophilicity.'' *RSC Adv.*, **3** (3) 671–690 (2013)